Articles

Analysis of Antibody A6 Binding to the Extracellular Interferon γ Receptor α-Chain by Alanine-Scanning Mutagenesis and Random Mutagenesis with Phage Display†

Stefan Lang,‡ Jian Xu,‡ Fiona Stuart,‡ Richard M. Thomas,§ Jan W. Vrijbloed,‡ and John A. Robinson*,‡

Institute of Organic Chemistry, University of Zürich, Winterthurerstrasse 190, 8057 Zürich, and Department of Polymer Chemistry, ETH-Zurich, Switzerland

Received April 13, 2000; Revised Manuscript Received August 3, 2000

ABSTRACT: The monoclonal antibody A6 binds a conformational epitope comprising mainly the CC′ surface loop on the N-terminal fibronectin type-III domain of the extracellular interferon γ receptor (IFNγR). The crystal structure of an A6 Fab−IFNγR complex revealed an interface rich in the aromatic side chains of Trp, Tyr, and His residues. These aromatic side chains appear to interact with both polar and hydrophobic groups at the interface, a property which, in general, may be advantageous for ligand binding. To analyze these interactions in more detail, the affinities of 19 A6 alanine-scanning mutants for the IFNγR have been measured, using engineered A6 single chain variable region fragments, and a surface plasmon resonance biosensor. Energetically important side chains ($\Delta G_{mutant} - \Delta G_{wt} > 2.4$ kcal/mol), that form distinct hot spots in the binding interface, have been identified on both proteins. These include V_LW92 in A6, whose benzenoid ring appears well situated for a π-cation (or π-amine) interaction with the side chain of receptor residue K47 and simultaneously for T-stacking onto the indole ring of W82 in the receptor. At another site, energetically important residues V_HW52 and V_HW53, as well as V_HD54 and V_HD56, surround the aliphatic side chain of the hot receptor residue K52. Taken together, the results show that side chains distributed across the interface, including many aromatic ones, make key energetic contributions to binding. In addition, the receptor CC′ loop has been subjected to random mutagenesis, and receptor mutants with high affinity for A6 have been selected by phage display. Residues previously identified as important for receptor binding to A6 were conserved in the clones isolated. Some mutants, however, showed a much improved affinity for A6, due to changes at Glu55, a residue that appeared to be energetically unimportant for binding the antibody by alanine-scanning mutagenesis. An E55P receptor mutant bound A6 with a 600-fold increase in affinity ($K_D \approx 20$ pM), which is one of the largest improvements in affinity from a single point mutation reported so far at any protein−protein interface.

The extracellular portion of the interferon γ receptor α-chain (*1*) (IFNγR)[1] comprises two FBN-III domains that together are responsible for binding IFNγ at the cell surface. The crystal structure of a complex formed between the neutralizing murine mAb A6 and the N-terminal FBN-III domain showed that the surface of the receptor contacted by A6 overlaps significantly with that bound by IFNγ in the ligand−receptor complex (*2*, *3*). The A6 epitope encompasses largely the CC′ hairpin loop on the receptor, although contact is also made with the neighboring F-strand (Figure 1). The antigen−antibody interface buries ca. 1660 Å^2 of protein surface, which includes 22 antibody residues from 5 CDRs and 11 residues from the receptor.

Antibody−antigen complexes remain interesting targets for mechanistic studies of protein−protein recognition, not least because high-affinity protein−protein interactions underlie many important processes in biology. Such studies are also of interest in the context of designing proteins, and smaller molecules, with novel recognition sites. One feature of interest in this case is the high concentration of aromatic groups (six Tyr, six Trp, and one His) located at the A6-IFNγR interface (four in V_L, six in V_H, and three in the receptor). This reflects a broader tendency for aromatic

† The authors thanks the Swiss National Science Foundation for financial support.

* To whom correspondence should be addressed. Phone: (++)-41-1-635-4242. Fax: (++)-41-1-635-6812. E-mail: robinson@oci.unizh.ch.

‡ University of Zürich. S.L., J.X., F.S., and J.V. all contributed equally to this work.

§ Department of Polymer Chemistry.

[1] Abbreviations: amp, ampicillin; CDR, complementarity determining region; FBN-III, fibronectin type-III domain; IFNγ, human interferon γ; IFNγR, extracellular portion (residues 1−229) of the human interferon γ receptor α-chain; mAb, monoclonal antibody; nt, nucleotides(s); scFv, single chain variable region fragment [$V_H + V_L$ joined by a $(G_4S)_3$ linker]; tet, tetracycline; Trx, *E. coli* thioredoxin; V_H, heavy chain variable region (residues are labeled, e.g., V_HW96); V_L, light chain variable region (residues are labeled, e.g., V_LR108); wt, wild-type.

10.1021/bi000838z CCC: $19.00
Published on Web 12/01/2000

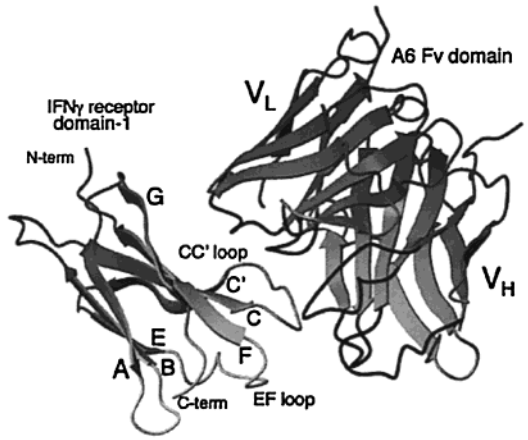

FIGURE 1: Ribbon diagram of the IFNγR$^{1-108}$-A6 Fab complex (*2*). The Fv (V_H + V_L) region of A6 is shown complexed to the N-terminal FBN-III domain of the receptor (PDB file 1JRH).

groups to be over-represented statistically in antigen binding sites on antibodies (*4*, *5*) and also, more generally, at protein−protein interfaces (*6*−*8*). The crystal structure of the A6-IFNγR complex reveals several aromatic rings which might participate in multiple types of interaction simultaneously, a property that may be relevant to their frequent occurrence in antigen binding sites. The energetic importance of such interactions is, therefore, of considerable interest.

We describe here new data on the contribution to binding affinity of antibody side chains buried at the A6-IFNγR interface, which complements earlier studies involving mutagenesis of the receptor (*9*). An experimental system for the study of an A6 scFv fragment is described, together with affinity measurements of scFv alanine-scanning mutants (*10*) using a surface plasmon resonance biosensor (BIACORE, Biacore AB). In addition, the receptor CC′ loop has been subjected to random mutagenesis and receptor mutants have been selected by phage display that have almost 3 orders of magnitude higher affinity for A6 than the wt. In particular, an E55P mutant has an approximately 600-fold higher affinity for the antibody, although the residue Glu55 appeared by alanine-scanning mutagenesis to be energetically unimportant for binding to the antibody.

EXPERIMENTAL SECTION

General. DNA and protein manipulations were as described in ref *11*.

Production of IFNγR with an Engineered C-Terminal Cys. The phagemid pOCI656 described earlier (*2*) was used as template DNA in a PCR with the primers: left 1, 5′-GGATTGTTATTACTCGCGGC-3′; right 1: 5′-TTCTGCGGCCGC*CTAACA*AGAACCTTTTATACTGC-3′.

The left 1 primer binds to a sequence upstream of the *Sfi*I and *Nco*I sites, present also in the parent phagemid pHEN1 (*12*). The right 1 primer (*Not*I site underlined; Cys and stop codons in italics) encodes the C-terminus of the receptor on the complementary strand, i.e., ...Ser^{224}-Ser^{225}-Ile^{226}-Lys^{227}-Gly^{228}-Ser^{229}-Cys-stop. When the PelB signal peptide is cleaved, the receptor from Glu^1-Met^2-Gly^3... to Ser^{229} with an additional Cys residue after Ser^{229} is produced and secreted into the *Escherichia coli* periplasm. The PCR product was digested with *Not*I and *Nco*I and cloned into *Nco*I/*Not*I digested pHEN1 to give pOCI1110. The nt sequence of the insert was confirmed by DNA sequencing.

Plasmid pOCI1110 was introduced into *E. coli* HB2151. The recombinant receptor was produced using a method described earlier (*2*), except that after the periplasmic extraction, β-mercaptoethanol (5 mM) was added to all buffers, and purification included immunoaffinity chromatography with antibody A6 coupled to CNBr-activated Sepharose (Pharmacia). After purification, the receptor was homogeneous by SDS−PAGE, gave an electrospray mass spectrum consistent with the calculated mass (25 970 Da), and the correct N-terminal sequence by Edman degradation. The protein was stable for at least 2 months at 4 °C in BIACORE buffer [sodium phosphate (50 mM), pH 7.2, NaCl (150 mM) and 0.005% (v/v) surfactant p20] containing β-mercaptoethanol (5 mM) and EDTA (5 mM). Upon prolonged storage, proteolysis led to the partial loss of the five N-terminal residues. This did not appear to affect recognition by A6.

Production and Characterization of A6 wt scFv. The primers left 1 and right 2 were used in a PCR with phagemid pOCI455 (*13*) as template: right 2, 5′-CCGGAATTCGCGGCCGCTTACCGTTTCAGCTCCAGCTTGGTC-3′.

The primer right 2 encodes, on the complementary strand, the C-terminus of V_L up to V_LR108 (*14*) followed immediately by a stop codon (underlined) and further downstream an *Eco*RI site (underlined). The PCR product was digested with *Sfi*I and *Eco*RI and cloned between the same sites in the vector pHB110 (*15*) to produce pOCI1103. This encodes a PelB leader sequence fused to the N-terminus of V_H, followed by the $(G_4S)_3$ linker, and V_L up to and including V_LR108. The leader peptide is cleaved during transport into the periplasm to give A6 scFv with residues Q^{1}V^{2}K^3... at the N-terminus.

The A6 scFv was produced by minor modifications to methods described earlier (*13*). The plasmid pOCI1103 was introduced into *E. coli* HB2151. The IPTG concentration for induction was 1 mM, and after induction, growth was at 26 °C for ca. 16 h. A periplasmic extract was made using a method described earlier for production of the IFNγR (*2*). The A6 scFv was purified by immunoaffinity chromatography with Trx-IFNγR$^{1-108}$ (*16*) coupled to CNBr-activated Sepharose, as described earlier (*13*). The protein from this column was applied to a MonoS ion-exchange column (Pharmacia) equilibrated in sodium phosphate buffer (50 mM, pH 6.8). The nativelike scFv eluted in the flow-through, whereas impurities could be eluted from the column in a salt gradient (0 to 0.5 M NaCl). The resulting protein showed a single band by SDS−PAGE, gave an electrospray mass spectrum consistent with the calculated mass, and the correct N-terminal sequence by Edman degradation.

The concentration of A6 scFv in PBS buffer [sodium phosphate 50 mM, NaCl (150 mM), pH 7.4] was determined by absorption at 280 nm (A_{280}), using A_{280} = 2.9 mg mL^{-1} after calibration by quantitative amino acid analysis. Gel filtration chromatography of A6 scFv was in PBS buffer on a TSK-GEL G3000SW column (7.5 × 600 mm) (Tosohass, Stuttgart) at a flow rate of 0.7 mL/min. CD spectra were recorded in PBS buffer using a Jasco J720 instrument at 25 °C. Analytical ultracentrifugation was performed using a Beckman XL-A instrument at 5 °C and 25 °C, at both 0.5 and 5 μM protein concentration in PBS buffer, at a rotor speed of 22 000 rpm. Data were acquired by averaging 20 radial scans at a spacing of 0.001 cm, and analyzed assuming

a single homogeneous species according to (eq 1)

$$c_r = c_o \exp[M_r(1 - \nu\rho)\omega^2(r^2 - r_o^2)]/2RT \qquad (1)$$

where c_r is the concentration of the protein at a given radial position, c_o is the concentration at a reference position, M_r is the apparent molecular weight, ν is the partial specific volume, ρ is the solvent density, ω is the angular velocity, r and r_o are radial positions (in cm) at an arbitrary position and at the meniscus, respectively, R is the gas constant, and T the absolute temperature.

Production of Mutant scFv. Mutations were introduced into the cDNA encoding the scFv by PCR with a mutagenic primer, using the method described earlier for mutagenesis of the receptor (*9*). The mutant scFvs were produced and purified by the same method used for the wt protein (see above), but also included gel filtration chromatography (see above). Each mutant showed one band of ca. 26 kDa on SDS−PAGE. CD spectra were recorded as for the wt (see above).

BIACORE Binding Assays. The IFNγR$^{1-229}$ containing a C-terminal *c-myc* tag, produced and purified as described earlier (*9*), was immobilized on a CM5 sensor surface (Biacore AB) by random amine coupling, using a method described earlier (*2*).

The IFNγR$^{1-229}$ with an engineered Cys residue near the C-terminus (see above) was immobilized on CM5 sensor surfaces by thiol exchange. The surface was activated by injection of N-hydroxysuccinimide (50 mM) and *N*-ethyl-*N*′-(dimethylaminopropyl)carbodiimide (200 mM) in water for 3 min, followed by 2-(2-pyridinyldithio)ethylamine (80 mM) in borate buffer (0.1 M, pH 8.5) for 1 min, and then Cys-containing IFNγR$^{1-229}$ (20 μg/mL) in sodium acetate buffer (10 mM, pH 4.0) for 2 min. Excess disulfides were blocked by injecting cysteine (50 mM) in formate buffer (0.1 M, pH 4.3) containing NaCl (1 M).

Binding curves were measured in BIACORE buffer at 25 °C. Association constants (K_A) were determined under equilibrium conditions from Scatchard plots according to the following equation (*17*, *18*):

$$R_{eq}/C = K_A(R_{max} - R_{eq}) \qquad (2)$$

where R_{eq} is the steady-state response, C is the protein concentration in the flow buffer, and R_{max} is the maximum surface binding capacity. K_A can be derived from the gradient of a plot of R_{eq}/C versus R_{eq} at different analyte concentrations (C). The standard deviation of the K_A determination upon repeated measurement with the same protein sample was typically ±5%. For kinetic analyses, an equation for a simple 1:1 interaction (eq 3) was fitted globally to binding curves collected at various analyte concentrations using the BIAevaluation software (v.3.0) (Biacore AB) (*19*):

$$dR/dt = k_{on}C(R_{max} - R) - k_{off}R \qquad (3)$$

where R is the response in RU and k_{on} and k_{off} are the association and dissociation rate constants.

Construction of pOCI1009. A PCR reaction was performed using the oligonucleotides primer 1 and primer 2 (see Table 1 in Supporting Information) and pOCI656 (*2*) as template DNA. A DNA fragment of the expected size (ca. 300 bp) was isolated by gel electrophoresis, digested with *Not*I and *Cla*I and subsequently ligated in *Not*I and *Cla*I digested pOCI656, to afford pOCI1009 (Figure 2). The nt sequence was confirmed by DNA sequencing.

Table 1: Alanine-Scanning Mutants Studied in This Work, the Measured Dissociation Constants (K_D), the Ratio of K_ds for Mutant and wt ($\Delta\Delta G = RT \ln(K_{mut}/K_{wt})$)

mutant	K_D (nM)	K_D(mut)/K_D(wt)	$\Delta\Delta G$ (kcal/mol)
wild-type	12 ± 0.3		
V_LE27A	30 ± 0.9	2.5	0.54
V_LD28A	25 ± 0.4	2.1	0.44
V_LY30A	78 ± 7	6.5	1.1
V_LY91A	32 ± 1.5	2.7	0.58
V_LW92A	1400 ± 80	117	2.8
V_LS93A	4 ± 0.2	0.33	−0.65
V_LT94A	23 ± 0.5	1.9	0.38
V_LW96A	200 ± 100	17	1.7
V_HY32A	135 ± 6	11.3	1.4
V_HW52A	1122 ± 35	94	2.7
V_HW53A	716 ± 50	60	2.4
V_HD54A	290 ± 30	24	1.9
V_HD55A	200 ± 50	17	1.7
V_HD56A	275 ± 5	23	1.8
V_HY58A	100 ± 3	8.3	1.2
V_HR95A	30 ± 2	2.5	0.54
V_HF98A	12 ± 0.3	1.0	0
V_HY99A	72 ± 5	6.0	1.1
V_HH100bA	211 ± 5	18	1.7

Preparation of Control Phage. A tetracycline resistance gene was excised from pBR322 on a 1.4 kb *Eco*RI−*Ava*I fragment and the 5′ ends were blunted using the Klenow fragment of PolI. The fragment was ligated in *Dra*I digested pHEN1 (*12*) to afford pOCI1005. The ampicillin (amp) resistance gene of pHEN1 is removed from the plasmid by the *Dra*I digestion.

ELISA Phage Panning. The method for phage panning was modified from (*20*). ELISA plates were coated overnight at 4 °C with mAb A6 (200 μL of 10 μg/mL). After washing three times with phosphate buffered saline [PBS; sodium phosphate, 50 mM, pH 7.2, and NaCl (150 mM)], the wells were incubated with PBS containing 1% BSA (200 μL) and incubated 2 h at 37 °C. The ELISA plate was washed again three times with PBS and finally the phagemid particles (ca. 10^9) were added in PBS containing 1% BSA and the plate was incubated overnight at 4 °C. The wells were washed 25 times with PBS containing 0.1% Tween 20, and 15 times with PBS, incubated 30 min at 20 °C, and finally washed 10 times with PBS. Bound phagemid particles were eluted with glycine buffer (200 μL, 50 mM, pH 2.5). The eluted material was neutralized with phosphate buffer (2 M, pH 7.5) and used for transfection of logarithmic growing *E. coli* XL1-blue cells.

Library Construction. A PCR was performed with the oligonucleotides primer 3 and primer 4 (see Table 1 in Supporting Information) and pOCI1009 as template. The product of the PCR was gel purified and used together with primer 5 in a second PCR again using pOCI1009 as template DNA. The resulting PCR product (ca. 800 bp) was gel purified, digested with *Nco*I, *Not*I, and cloned in *Nco*I/*Not*I digested pOCI1009, yielding plasmid pOCI1010 in which the cDNA encoding the central portion of the CC′ receptor loop has been deleted (Figure 2).

To construct the libraries, cassettes were prepared by annealing oligo 1 with oligo 2, oligo 3 with oligo 4, and

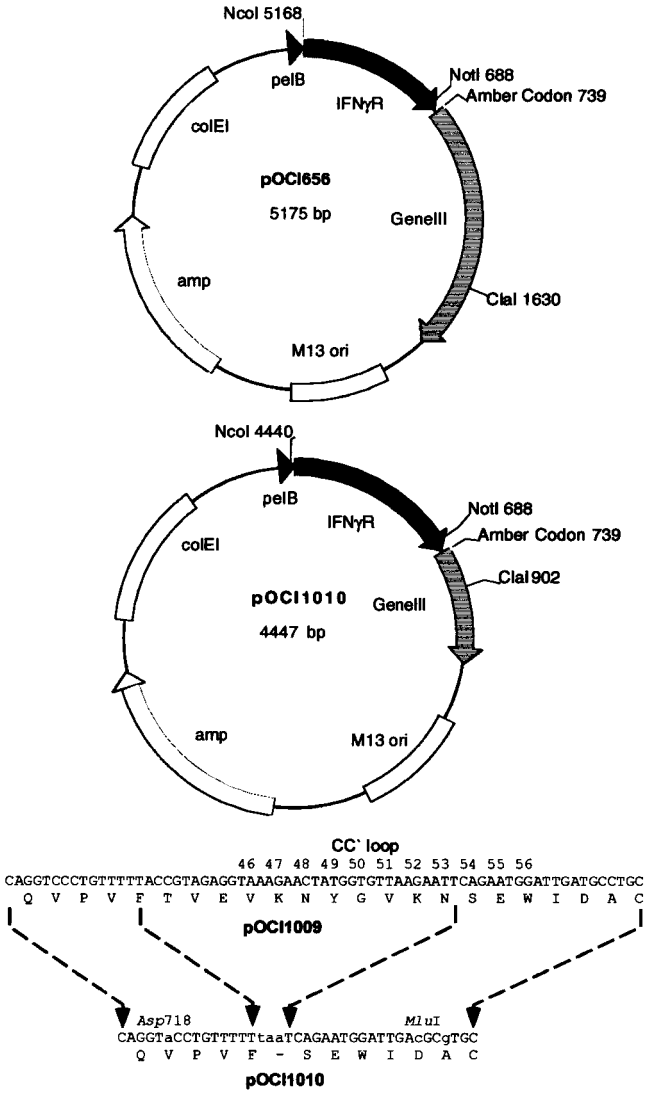

FIGURE 2: Phagemids pOCI656 and pOCI1010. Below is shown the nt sequence of the CC′ loop region in the wt state (in pOCI1009), and after modification as in pOCI1010. The dotted lines indicate corresponding positions in the nt sequence in each clone, and show how the segment encoding the central part of the loop was deleted in pOCI1010 (see Experimental Section and Results). Oligonucleotide cassettes encoding the mutant libraries were ligated into *Asp*718/*Mlu*I digested pOCI1010.

oligo 5 with oligo 6 (see Table 1 in Supporting Information). A total of 31.9 pmol of each of the six oligonucleotides was annealed in the appropriate combinations by 5 min heating at 95 °C and slowly cooling to 30 °C (30 min). The complementary strands were synthesized by extension of the 3′ ends by adding 1 mM dNTP and 20 units of klenow fragment of *Pol*I and continued incubation at 30 °C for 1 h. The resulting double-stranded DNA was digested with *Asp*718 and *Mlu*I and then ligated in *Asp*718 and *Mlu*I digested pOCI1010. Introduction of the ligated DNA into *E. coli* XL1-blue cells was by electroporation using a genepulser (Bio-Rad). Colonies were pooled in fractions and frozen in 20% glycerol.

Preparation of Phage. Frozen stocks were used to inoculate 2YT (25 mL) containing 1% glucose and ampicillin (100 μg/mL). The culture was grown for 4 h at 37 °C and the cells were pelleted by centrifugation (4000 rpm) and washed once with 2YT. The cells were resuspended in 2YT and M13KO7 phage was added at a multiplicity of infection of 40. After 20 min incubation at 37 °C without shaking, incubation was continued for 1 h at 37 °C with shaking. Then kanamycin (20 μg/mL) was added to the culture, which was 20-fold diluted in fresh 2YT containing ampicillin (100 μg/mL) and kanamycin (20 μg/mL) and grown overnight at 37 °C.

Glycine-eluted phage obtained after a round of panning was directly used to infect logarithmic growing *E. coli* XL1-blue. The cells were pregrown on 2YT containing 1% glucose to an OD_{600} of 1.0. After 20 min incubation at 37 °C without shaking, incubation was continued at 37 °C with shaking for 1 h. At this point ampicillin (100 μg/mL) was added to the culture and incubation was continued for 4 h at 37 °C. Infected cells were harvested by centrifugation at 4000 rpm and the cell pellet was resuspended in 2YT containing ampicillin (100 μg/mL). Infection by M13KO7 phage was as described above. Phagemid particles from liquid cultures were obtained as described by (*21*).

Production of Mutant Receptor Proteins. The E55P mutant IFNγR$^{1-229}$ cDNA was prepared by site-specific mutagenesis and PCR using methods described elsewhere (*9*). Production and purification of wt IFNγR and mutant proteins, each fused to a C-terminal *c-myc* tag, was as described previously (*2*). For competition BIACORE, proteins were produced that lacked the *c-myc* tag, and these were purified by immunoaffinity chromatography with A6. The homogeneity of purified proteins were confirmed (>95%) by SDS−PAGE, and the masses by electrospray mass spectrometry.

Competition ELISA. K_Ds of the wt IFNγR and mutant proteins binding to A6 were determined by competition ELISA as described earlier (*9*).

Competition BIACORE Measurements. The wt IFNγR$^{1-229}$ was immobilized on CM5 sensor surfaces by random amine coupling, as described earlier (*2*). The level of immobilized receptor corresponded to ≥10 000 RU. The wt A6 scFv together with various concentrations of wt IFNγR$^{1-229}$ were preincubated for at least 1 h at 4 °C, before injection over the IFNγR$^{1-229}$-sensor surface (flow rate 25 μL/min, injection volume 150 μL). At least 10 binding curves with different concentrations of IFNγR$^{1-229}$ were measured. Each measurement was performed at least in duplicate. The slopes of the association phases were determined using BIAevaluation, software v.3.0, and were plotted against the total antigen concentration. The K_D was determined by fitting to eq 4 (*22*) using KALEIDAGRAPH (Synergy Software, PA):

$$r_{obs} = r_{max}\left(1 - \frac{1}{[Ab_{tot}]}\cdot\left(\frac{K_D + [Ag_{tot}] + [Ab_{tot}]}{2} - \sqrt{\left(\frac{K_D + [Ag_{tot}] + [Ab_{tot}]}{2}\right)^2 - [Ag_{tot}][Ab_{tot}]}\right)\right) \quad (4)$$

where r_{obs} is the slope at a given $[Ag_{tot}]$, r_{max} is the maximal slope in the absence of inhibition by co-incubated antigen, $[Ab_{tot}]$ is the total scFv concentration, $[Ag_{tot}]$ is the total antigen concentration, and K_D is the dissociation constant.

RESULTS

Expression of Extracellular IFNγR. The wt IFNγR, residues 1−229 (IFNγR$^{1-229}$), fused at the C-terminus via a short -Ala$_3$- linker to a *c-myc* peptide tag (*23*), was produced

in *E. coli* using a secretion expression system described earlier (*2*). IFNγR$^{1-229}$ with a cysteine residue engineered at the C-terminus (but without the *c-myc* tag) was produced in the same way. Both proteins were purified by immunoaffinity chromatography, using either immobilized A6 mAb or the 9E10 mAb against the *c-myc* tag (*23*).

Expression and Properties of A6 scFv. The A6 scFv fragment comprising the V_H domain connected through a linker [$(G_4S)_3$] to the V_L chain with a *c-myc* tag attached to the C-terminus (yield $\approx$ 0.3 mg/L), was produced and purified as described earlier (*13*). However, the yields of some A6 mutants made in this way were much lower, so an improved expression system was implemented. The wt A6 scFv coding region was cloned into vector pHB110, which also contains the *E. coli skp* gene (*15*). After purification, the scFv was obtained in a yield of ~1.2 mg/L. Eleven of the 19 mutants were obtained in the same way in about the same yield as wt, the V_HH100bA, V_LW92A, V_LY91A, V_HD54A, and V_LW96A mutants were obtained in 5−6-fold lower yield, and the V_HW53A, V_HW52A and V_HD55A mutants in ~10-fold lower yields.

When micromolar solutions of wt A6 scFv were diluted to 100 nM and injected over a biosensor surface displaying immobilized IFNγR, the shape of the binding curve was seen to change with elapsed time (over ~60 min) after dilution from the stock solution (data not shown). Freshly diluted sample gave a pronounced biphasic binding curve with a significant contribution from a component with a very slow dissociation rate. The binding curves at later times resembled those typical for a 1:1 interaction with a fast dissociating species. Such behavior could be explained by a dynamic equilibrium between monomeric and multimeric forms of A6 scFv. Upon sedimentation equilibrium analytical ultracentrifugation, the fit of a model which assumed a single molecular species to the sedimentation data was influenced by the temperature and the protein concentration. At a higher protein concentration (5 μM) and 5 °C, the apparent molecular weight was higher than expected and the fitting was poor. A 10-fold dilution to 0.5 μM and measurement at 25 °C, however, gave a molecular weight determination (27.9 kDa) close to the calculated mass with good fitting of the model (Figure 3). Gel filtration chromatography of A6 scFv at high protein concentrations also indicated the presence of dimer, which disappeared from chromatograms upon dilution of the scFv to <1μM protein concentration (data not shown).

Data from gel filtration, analytical ultracentrifugation and biosensor measurements provide mutually supportive evidence that the wt A6 scFv has a tendency to dimerize at high concentrations. The propensity of scFvs to dimerize is well-known, and has been demonstrated for several different antibody fragments (*20*, *24*−*29*).

The CD spectrum of the wt scFv (Figure 4) shows a trough at 219 nm with a change to positive ellipticity below 211 nm, which is typical of all-β-proteins (*30*). A positive band is seen at 233 nm, which is indicative of an exciton couplet. Two pairs of Trp side chains have closely neighboring indole rings, V_HW47 with V_LW96, and V_HW53 with V_HW52. In CD spectra of scFv mutants V_LW96A, V_HW52A, and V_HW53A, the positive peak at 233 nm is significantly reduced in intensity relative to the band at 219 nm, consistent with one or both of these Trp pairs being responsible for the exciton couplet. In the near-UV CD spectrum of wt scFv, a weak positive peak at 272 nm is also found (not shown).

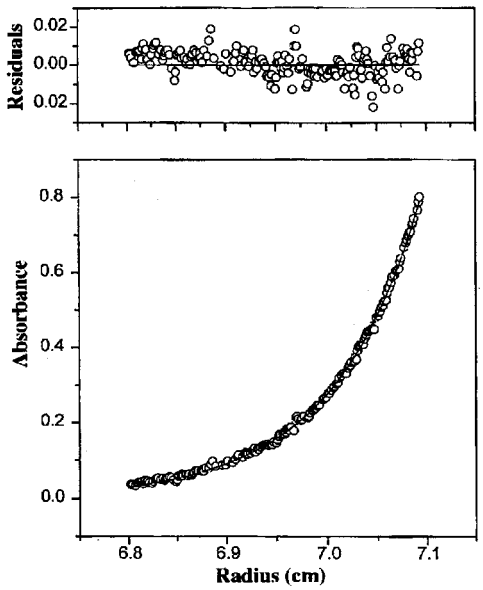

FIGURE 3: Sedimentation equilibrium analytical ultracentrifugation data obtained for the A6 scFv at 0.5 μM concentration and 25 °C. The residuals indicate the deviation of the data points from the fitted curve (see Experimental Section).

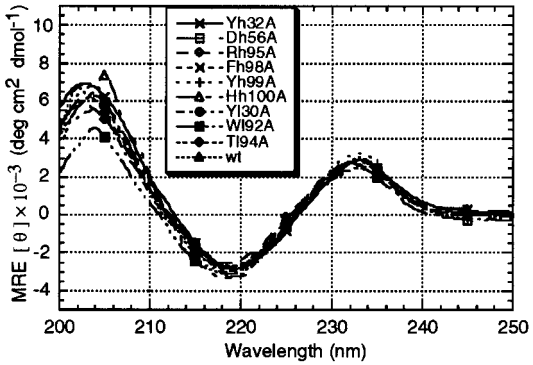

FIGURE 4: CD spectra of wt and several mutants of the A6 scFv. From the overlay it is apparent that the CD spectra of wt and mutants are all very similar to each other.

The far-UV CD spectra of most other scFv mutants (except V_LY91A, V_HD54A, and V_HD55A, which were not measured) were similar to that of the wt scFv (Figure 4). This group includes mutants that show large changes in K_D for the receptor (e.g., V_LW92A, V_HH100bA, V_HD56A) as well as others where the K_D is little changed (V_LT94A and V_HF98A). The mutants V_LS93A, V_LE27A, V_LD28A, and V_HY58A, whose K_Ds were also not significantly changed, showed small differences in the relative intensity of the positive ellipticity at 205 nm compared to wt.

The CD spectra indicate that the wt immunoglobulin fold is retained in the mutants, although local changes in conformation of the CDR loops cannot be ruled out.

Biosensor Measurements with wt scFv. In a first series of experiments, the IFNγR$^{1-229}$ protein with a *c-myc* tag at the C-terminus was immobilized on the biosensor surface by random amine coupling. Monomeric scFv was purified by gel filtration, and the absence of dimer in the resulting protein was confirmed upon rechromatography. When the scFv concentration was varied in the range 3−100 nM, the binding

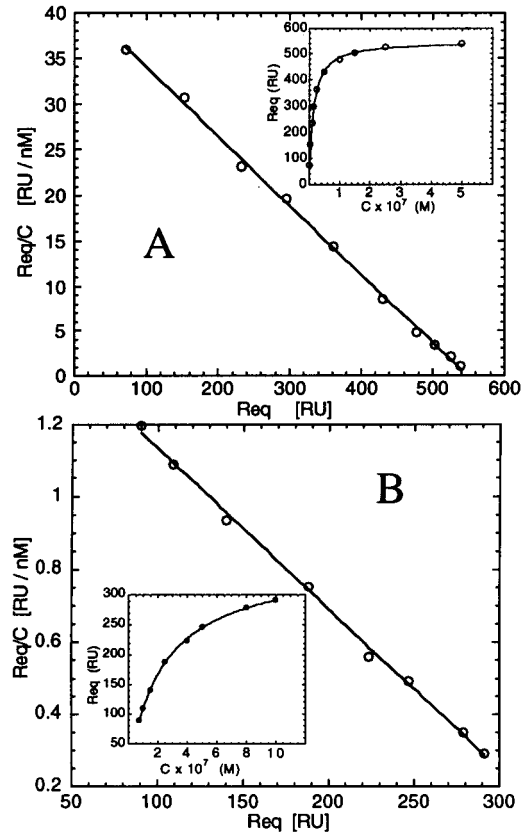

FIGURE 5: (A) Scatchard plot of the binding data from biosensor measurements with the wt A6 scFv. Inset is the same data presented as a plot of equilibrium sensor response (R_{eq}) against analyte concentration (M). B, is the same treatment of data for the V_H-H100bA mutant.

curves gave linear Scatchard plots and a K_D of 12 nM. A kinetic analysis of the data gave an apparent k_{on} of 1.1×10^6 M^{-1} s^{-1} and an apparent k_{off} of 1.4×10^{-2} s^{-1}. A linear Scatchard plot was also obtained from data on the binding of IFNγR$^{1-229}$ protein to immobilized A6 mAb, and the measured K_Ds were 13 and 15 nM (composed of $k_{on} = 6.1 \times 10^5$ M^{-1} s^{-1} and $k_{off} = 0.87 \times 10^{-2}$ s^{-1}) from steady state and kinetic analyses, respectively. Determination of apparent k_{on} and k_{off} values using three different densities of immobilized IFNγR$^{1-229}$ and three different flow rates showed that mass transport effects had little influence on binding under the conditions used to determine K_D values.

In a second series of experiments, IFNγR$^{1-229}$ with an engineered Cys at the C-terminus was immobilized on the biosensor surface through the free thiol. A steady-state analysis of scFv binding to this surface gave a linear Scatchard plot and a K_D of 12 nM (Figure 5). Hence, the random amine coupling procedure does not significantly affect the affinity of A6 for its epitope on the receptor.

Biosensor Measurements with scFv Mutants. Nineteen scFv mutants were prepared and their affinities to the receptor analyzed (Table 1). Since biosensor assays can be significantly affected by the presence of even small amounts of dimeric species (*31*), the mutant scFvs were purified by gel filtration prior to measurements with the BIACORE instrument, and where possible, the scFv concentration was kept below 500 nM. Dissociation constants (K_D) were determined by steady-state analyses from Scatchard plots (Table 1 and Figure 5). The K_D values measured in duplicate experiments were generally within ±20% of the mean value, the variation probably reflecting the accuracy of the determination. Only for several low affinity mutants was the standard deviation higher. For the wt scFv and some mutants, the association phase of the binding curves fitted well to a simple 1:1 binding model using global kinetic analysis, whereas, for other scFv mutants, significant biphasic association phases were apparent under all conditions examined.

Display of the IFNγR on Phage. The phagemid pOCI1009, encoding the extracellular IFNγR$^{1-229}$ cDNA fused to a truncated M13 gene III, was prepared such that the TAG amber stop codon of IFNγR was directly adjacent to codon 246 of M13 gene III. In this way two GGGGS repeats were placed between the IFNγR and the C-terminal domain of gene III protein.

The ability of the recombinant IFNγR-phage to bind to mAb A6 coated ELISA plates was assessed in competition with a control phage (pOCI1005) without the receptor but containing a tet resistance gene. After panning a 1:1 mixture of pOCI1009- and pOCI1005-phage particles on immobilized mAb A6, phage particles that displayed IFNγR (pOCI1009) were enriched about 60−100 fold over the control phages (pOCI1005). No specific enrichment of pOCI1009 was seen when an excess (1 μM) of mAb A6 or IFNγR was added to the starting phage mixture. These results indicated that correctly folded and functional IFNγR extracellular domains were present on the phage surface.

Library Construction. To facilitate random mutagenesis of the CC′ loop, the phagemid pOCI1009 was modified such that most of the DNA encoding the CC′ loop was deleted, a stop codon was introduced in the reading frame of IFNγR, and *Asp*718 and *Mlu*I restriction sites were introduced in the flanking regions (Figure 2). The resulting phagemid (pOCI1010) does not encode a functional wt receptor protein. Function can be restored by inserting a cassette between the *Asp*718 and *Mlu*I restriction sites that encodes a loop of the desired length with selected positions randomized.

Three separate libraries were constructed. In the first library, the receptor residues E45.V46.K47.N48.Y49 were randomized, in the second, receptor residues Y49.G50.V51.K52.N53, and in library three, residues N53.S54.E55.W56.I57. The three libraries together encompass the entire hairpin loop sequence bound by the A6 antibody (see Figure 11). Additional and different silent mutations in the nt sequence were also introduced into the flanking constant regions in each library as a distinguishing feature to allow detection of cross-contamination, although none was found.

The insert frequency for each library ranged from 86 to 93%. The codon usage determined from 105 clones was close to random with no large bias in the inserted nucleotides and no over representation of any specific codons. The sizes of the libraries ranged from 1.8×10^7 to 4.3×10^7 independent clones and were considered large enough to contain all or almost all of the possible protein sequences.

Phage Panning. Phage panning was carried out for four consecutive rounds. After the last round individual colonies were randomly chosen for nt sequencing. Approximately 50 clones from each library were sequenced and the deduced translated protein sequences are given in Table 2. A statistical

Table 2: Deduced Amino Acid Sequences of the Mutants Selected by Phage Panning[a]

Library-1			Library-2			Library-3		
EVKNY		Number	YGVKN		Number	NSEWI		Number
EHKWY		11	YGVKN		27	NSPWR	**	8
GVKSY	*	6	YGTKN	*	4	NGGWR	**	6
ENKWY		4	YGYKN	*	3	NSPWL	**	4
EAKSY	*	3	HGVKN	*	2	NTPWS	*	4
EAKTY	*	3	YGHKN	*	1	NAPWT	*	2
EEKRH		2	YGLKN	*	1	NGPWK	**	2
QAKSY	*	2	HGLKN	*	1	NPRWQ		2
AVKEY		2				NSPWV		1
QAKEY		1				NSPWA		1
EAKNY		1				NSPWS		1
EGKWY		1				NSPWF		1
EVKSY		1				NTPWV		1
ETKVY		1				NAPPN		1
EEKSY		1				NAPWE		1
EHKVY		1				NGPWV		1
EQKFY		1				NGPWR		1
EMKTY		1				NSVFH		1
KVKNY		1				NPSWS		1
MNKWH		1				NPTWT		1
GVKIH		1				NPTWQ		1
GLKTY		1				NPTYR		1
SVKSY		1				NPAYR		1
IAKSY		1				NPGWV		1
LVKTY		1				NPRWM		1
						NGLWT		1
						NGDYE		1
						NGSWR		1
						NGYYE		1
						NGTWR		1
Total 49			Total 39			Total		50

[a] The wt sequence, representing the region subjected to mutagenesis in each library, is shown at the top. The amino acid sequence of the entire CC′ hairpin loop on the wt receptor is $E^{45}V^{46}K^{47}N^{48}Y^{49}G^{50}V^{51}K^{52}N^{53}S^{54}E^{55}W^{56}I^{57}$. The number of times each sequence was found is also given, with the most frequently found at the top, and the total at the bottom. (*) K_D was determined by ELISA. (**) K_D was determined by ELISA and by competition BIAcore.

analysis of the occurrence of amino acid types at each position in each library is shown in Figure 6.

IFNγR Mutants. Several of the most frequently found mutant receptors in each library were produced as soluble proteins, as described for the wt receptor and in similar yields. The mutants EHKWY and ENKWY (from library 1, Table 2) could not be purified, as they were unstable upon acid elution from the 9E10 immunoaffinity column.

The affinity of mutant IFNγR for A6 was first assayed by competition ELISA, and apparent K_Ds were determined for mutants from libraries 1 and 2 (Figure 7). In the same assay, the mutant receptors recovered from library 3 possessed a 2−3 orders of magnitude higher affinity for A6 than the wt receptor. The single mutant E55P, although not isolated from library 3, was generated by site-specific mutagenesis, produced in *E. coli*, and its affinity for A6 was also shown by competition ELISA to be much higher than for the wt. For selected high-affinity mutants the K_Ds were determined by competition BIAcore (Figure 8 and Table 3). The results indicate an important effect of mutation at residue E55 on affinity to the antibody.

Binding of IFNγΔ10 [lacking the 10 C-terminal residues (*32*)] to wt IFNγR immobilized on the biosensor surface was compared to its binding to immobilized E55P mutant. Whereas the IFNγΔ10 bound to the wt receptor with approximately nanomolar affinity (data not shown), binding to the E55P mutant was largely abolished and could not be determined by BIACORE.

DISCUSSION

It is noteworthy that the results presented here interlock well with crystallographic data on the IFNγR−A6 complex (*2*), and with the results of earlier alanine-scanning mutagenesis studies on the receptor (*9*). Upon alanine-scanning mutagenesis of the A6 scFv, three mutations (V_LW92A, V_HW52A, and V_HW53A) are seen to have a large impact (2.4−2.8 kcal/mol) on affinity, nine others (V_LY30A, V_LW96A, V_HY32A, V_HD54A, V_HD55A, V_HD56A, V_HY58A, V_HY99A, and V_HH100bA) show significant effects (1−2 kcal/mol), while seven others (Table 1) have little or no effect (<1 kcal/mol). The three most important all involve Trp residues, and each of their side chains appears to be involved in multiple types of interaction. The benzenoid ring of V_LW92 appears well situated for a π-cation (or π-amine) interaction with the side chain CE and NZ atoms of receptor residue K47 [both atoms are ∼3.9 Å from the plane of the indole ring (*33*)] and for simultaneous T-stacking onto the indole ring of W82 in the receptor [5.1 Å between the ring centers shown in Figure 9A (*34*, *35*)]. The V_LW92 side chain, therefore, makes hydrophobic (with W82) and polar (with K47)

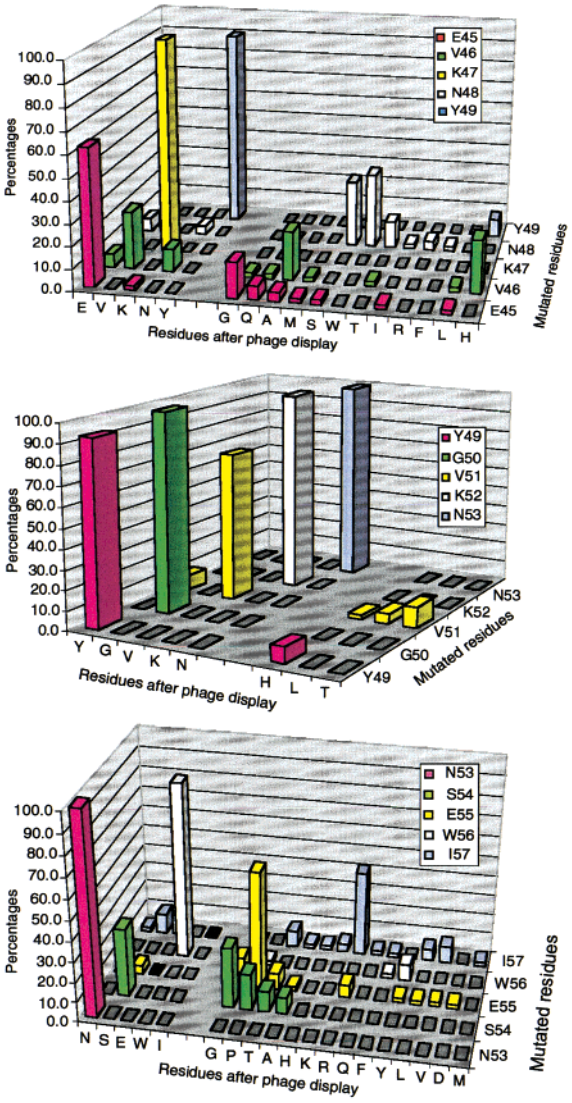

FIGURE 6: Bar diagrams showing the percentage occurrence of the amino acid types at each randomized position in the clones isolated from each library after panning on A6: (A) top = library 1; (B) middle = library 2; and (C) bottom = library 3. The data are taken from Table 2.

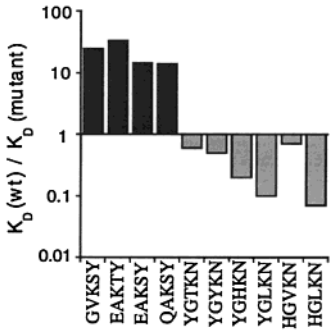

FIGURE 7: Results of ELISA to determine affinities for antibody A6 of mutant receptors isolated from libraries 1 (filled bars) and 2 (shaded bars). The affinity relative to the wt receptor [K_D (wt)/K_D (mutant)] is shown for each mutant.

contacts simultaneously with the receptor, although the relative importance of these and other interactions cannot presently be assessed. The receptor K47 and W82 side chains were identified earlier as being energetically important [affinity change relative to wt upon mutation to alanine, ~3.6 and 4.5 kcal/mol (*9*)].

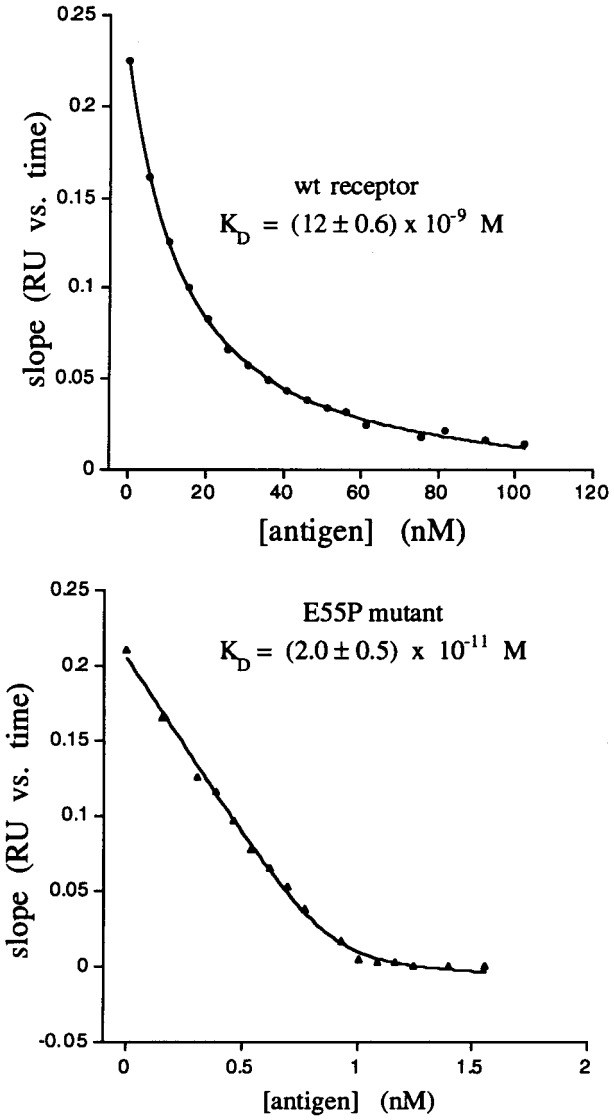

FIGURE 8: Competition BIACORE. Plots of the slope of the association phase vs corresponding total soluble antigen concentration. The lines represent the fitting to Eq 4 (Experimental Section). The calculated K_D for the wt (top) and single mutant E55P (bottom) are shown.

Table 3: Sequences of Mutant IFNγR$^{1-229}$ Proteins and Their K_Ds (± SD) for Binding to A6 scFv Determined by Competition BIAcore (see Figure 8)[a]

mutant	K_D (nM)	K_D(wt)/ K_D(mut)
NSEWI (wt)	12 ± 0.6	
NSPWR	0.036 ± 0.02	333
NGGWR	0.040 ± 0.003	300
NSPWL	0.035 ± 0.01	343
NGPWK	0.017 ± 0.007	706
NSPWI	0.020 ± 0.005	600

[a] The change in affinity relative to wt is also shown.

Two other hot residues in the antibody are V_HW52 and V_HW53, which together with V_HD54 and V_HD56, surround the aliphatic side chain of K52 (Figure 9B) [itself identified earlier as a hot residue in the receptor (*9*)]. Many of the mutations that exhibit significant effects (1−2 kcal/mol) (i.e., "warm spots") surround V_HW52 and V_HW53 (Figure 10). A similar observation of hot spots surrounded by warm

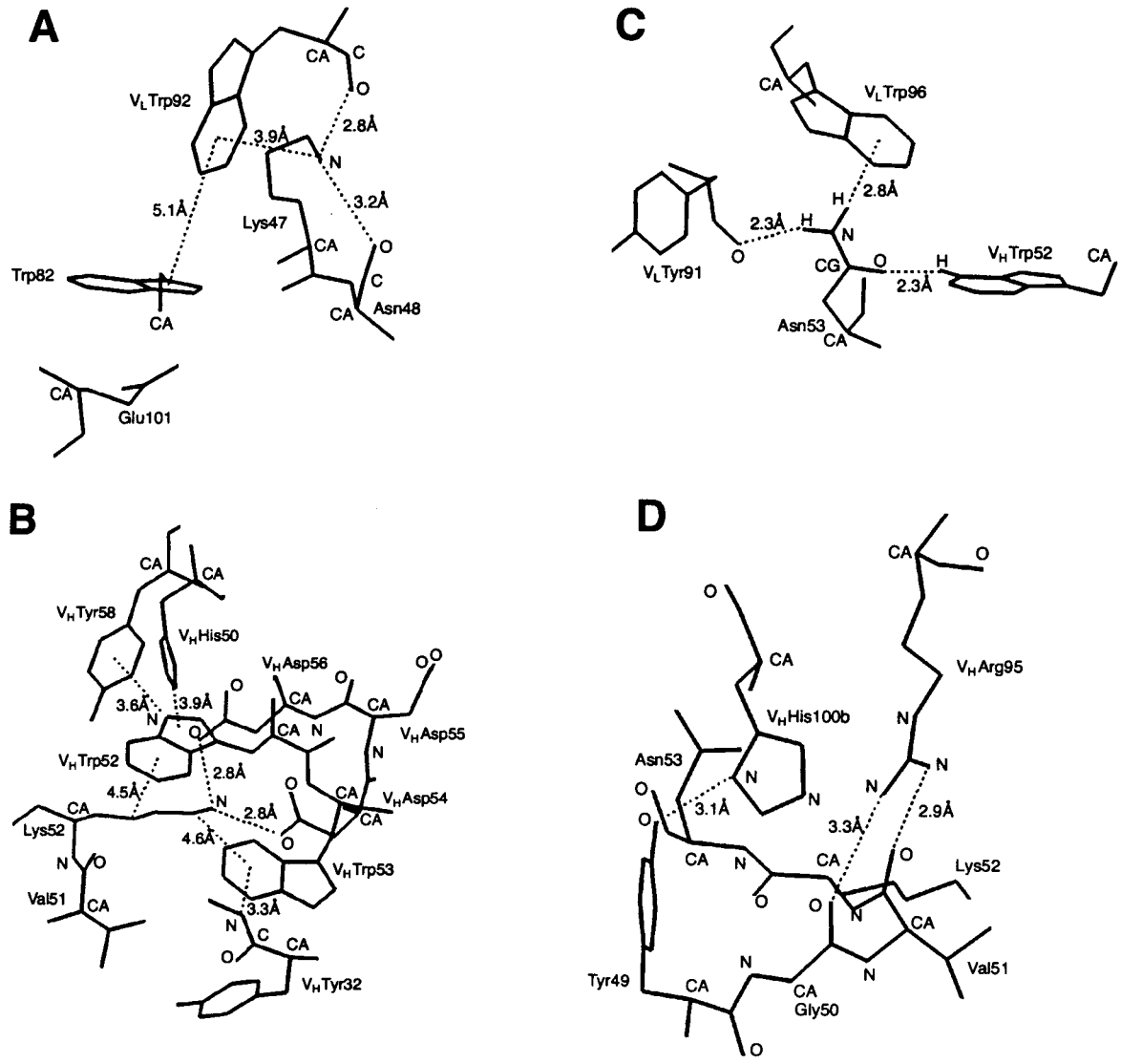

FIGURE 9: Line diagrams showing interacting residues at the A6-IFNγR$^{1-108}$ interface. (A) Receptor residues Lys47 and Trp82 interacting with V_LTrp92. Distances between the Lys47 side chain N atom and the center of the benzenoid ring of V_LTrp92, as well as between the ring centers of V_LTrp92 and Trp82 are shown. (B) Receptor residue Lys52 interacting with V_HTrp52 and surrounding residues. (C) Receptor residue Asn53 and surrounding antibody residues. (D) The receptor loop from Asn53 to Tyr49 situated below V_HHis100b and V_HArg95. Dotted lines indicate interactions mentioned in the Discussion.

residues was made in studies of the HyHEL-10-lysozyme complex (*36*). The side chain NZ atom of receptor K52 lies close to the side-chain carboxylate groups of both V_HD54 and V_HD56 in the antibody. Mutation of either of these two aspartate residues causes a significant loss in affinity, as does mutation of V_HD55 whose side chain points away from K52 toward bulk solvent (Figure 9B) (Table 1). One explanation for the effect of the V_HD55A mutation might be a change in the conformation or dynamics of the CDR loop. It is often unclear to what extent conformational effects influence alanine-scanning mutagenesis data, although such effects have often been discussed in the context of antibody−antigen binding. The indole of V_HW52 appears to participate in a dense network of interactions, since one face lies close to the four methylene groups of receptor K52, its indole NH T-stacks with the phenol ring of V_HY58, and its other face (not in contact with K52) T-stacks with the side-chain imidazole of V_HH50. Here also, the relative energetic importance of these interactions is presently unknown.

Residues Y49 and N53 have also been identified as hot residues on the receptor (*9*). The aromatic ring of Y49 fills a pocket formed between the V_H and V_L chains of A6. On the other hand, the side-chain amide NH_2 group of residue N53 appears to be well situated for H-bonding to the backbone carbonyl CO of V_LY91 and the indole ring of V_L-W96 (Figure 9C), and mutation of the latter does have a significant effect on affinity (Table 1).

The heavy chain residue V_HH100b is buried in the interface (Figure 9D), and its mutation to alanine also leads to a significant drop in affinity (Table 1). On the other hand, the buried guanidinium group of V_HR95A appears to H-bond to two backbone carbonyl CO groups of receptor residues G50 and V51 (Figure 9D), although removal of this Arg side chain results in only a small loss in affinity. This was unexpected since the mutation presumably removes two charged hydrogen bonding interactions.

In summary, the results of alanine-scanning mutagenesis of both the receptor and A6 reveal that multiple side chains

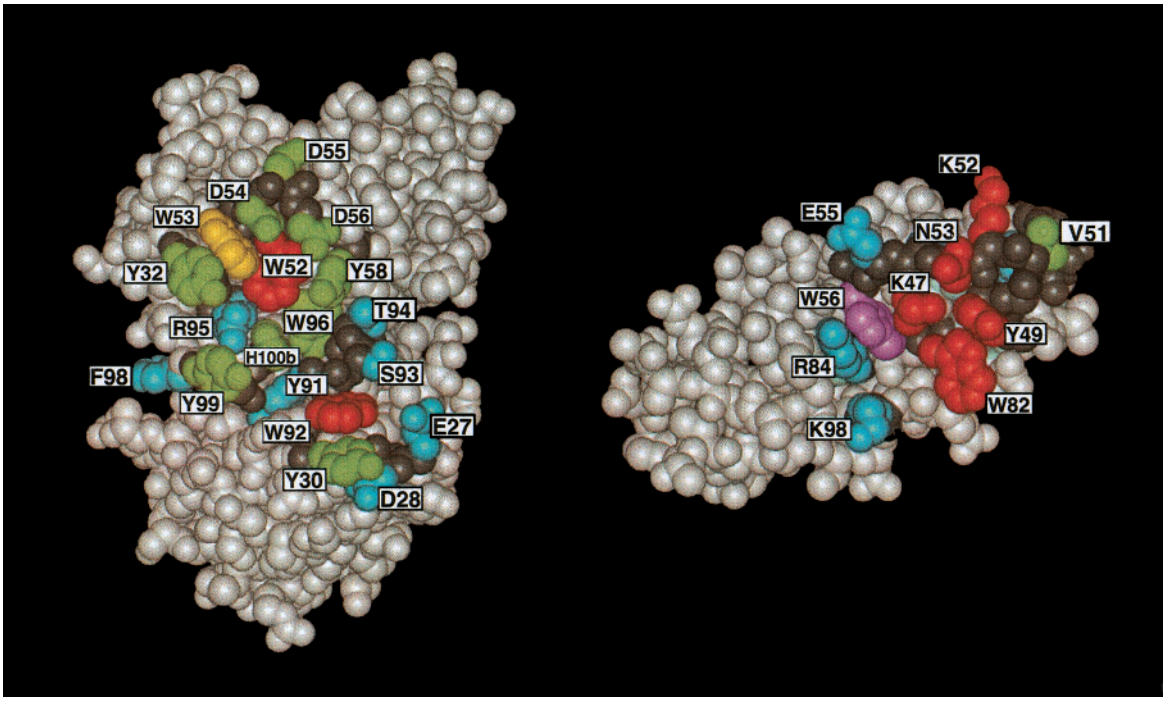

FIGURE 10: CPK representation of the interface, left looking onto the scFv, right looking onto the receptor. Folding the page vertically through the center illustrates how the interface is formed. The side chains of mutated residues are color coded, red = $\Delta\Delta G$ > 2.7 kcal/mol, yellow = $\Delta\Delta G$ 2.0−2.7 kcal/mol, green = $\Delta\Delta G$ 1.0−2.0 kcal/mol, and blue < 1.0 kcal/mol (see Table 1). The backbone atoms are in gray. The receptor residue W56 could not be replaced by alanine and is shown in pink (*9*).

contribute significantly to the energetics of binding, including both polar and aromatic ones, at different loci across the interface (Figure 10).

In some protein−protein complexes, relatively few productive interactions near the center of the interface dominate the energetics of association, as found, for example, in the growth hormone-receptor complex (*37*), the antibody D1.3-hen egg white lysozyme complex (*38*, *39*), and the HyHEL-10−lysozyme complex (*40*−*44*). In contrast, the stabilization of the D1.3−E5.2 antibody−antibody complex (*38*, *45*) is apparently achieved by the accumulation of several productive interactions of varying strength over the entire interface. This also appears to be the case for a VEGF−Fab interface, which is again rich in aromatic residues (*46*). However, in all these cases hot residues on one protein pack against hot residues on the other across the interface, as also found here for the A6−IFNγR complex.

Additional interesting information about the A6-IFNγR interface was obtained using phage display methods and random mutagenesis. Three libraries of mutants were prepared, in which the CC′ receptor loop was subjected to random mutagenesis in three five residue sections.

In the first library, the residues E45.V46.K47.N48.Y49 were randomly mutated (Figure 11), so that each position could be filled by any of the other 20 proteinogenic amino acids. This region includes residues K47 and Y49, which were shown by alanine-scanning mutagenesis to be energetically important (i.e., hot) side chains. These two hot residues, K47 and Y49, were highly conserved in the clones isolated. In only three different sequences was Y49 substituted by His (Figure 6). Unfortunately, two of the most abundant sequences recovered from this library (EHKWY and ENKWY) were refractory to purification as soluble proteins. Four other mutants were produced, however, and their

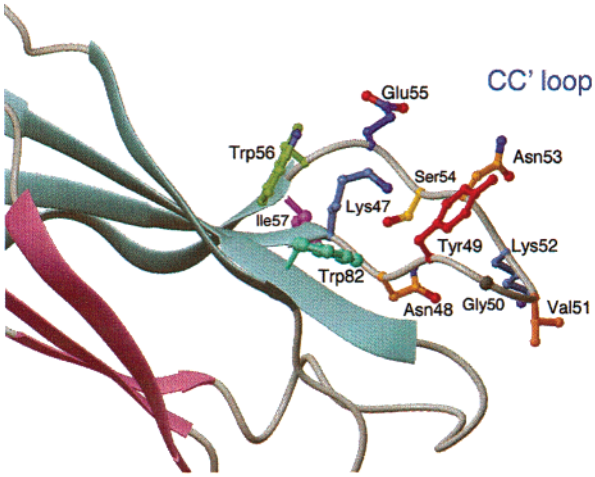

FIGURE 11: A6 epitope on the IFNγR (*2*).

affinities for A6, assayed by competition ELISA (Figure 7), were approximately an order of magnitude higher than seen for the wt. Since the changes occur in residues that do not make significant contact with the antibody (E45, V46, and N48), the origins of the improved affinities presumably lie in changes to the conformation of the epitope.

In the second library, the residues Y49.G50.V51.K52.N53 at the tip of the CC′ hairpin loop (Figure 11) were randomized. The hot residues Y49, K52, and N53 (*9*) were strictly conserved, as was G50 which is important for conserving the turn conformation at the tip of the loop (Figure 6, Table 2). The affinities of six receptor mutants from this library were shown by competition ELISA to be about the same or slightly lower than found for the wt (Figure 7).

In the third library, the residues N53.S54.E55.W56.I57 were randomly mutated (Figure 11). Residue N53 was strictly

conserved (Figure 6 and Table 2), consistent with its identification earlier as a hot residue (*9*). The W56 residue was also strongly conserved as either Trp, Tyr, or Phe. The remaining three positions in the β-strand showed more variability (Figure 6). S54 was in some cases replaced by a residue with a small polar, but noncharged side chain (G, T, A, or P). This side chain is largely buried under the CC′ loop in the antibody−antigen complex (Figure 11), which presumably restricts the size of group that can be accommodated at this position. A Glu residue was not found at position-55 in the recovered clones, but was most frequently substituted by Pro. In the A6-IFNγR complex, the E55 side chain is directed out from the CC′ loop toward bulk solvent. Earlier studies revealed that S54A and E55A mutants each have about the same or slightly improved affinity for A6 compared to wt (*9*). These side chains [beyond C(β)] appear, therefore, to be nonessential for recognition by A6. Position I57 in the library could be substituted by a variety of different residues, with a somewhat stronger preference for polar/charged residues (Figure 6). This is understandable, since the side chain of I57 points away from A6 into bulk solvent (Figure 11).

Six of the most frequently recovered clones from library 3 were produced as soluble proteins. Competition ELISA clearly showed that all six had a significantly improved affinity for A6 compared to the wt, by about 2−3 orders of magnitude (data not shown).

An alternative method of measuring the K_Ds of these mutants was investigated, since their affinities are at the upper limits for accurate quantification by ELISA, and kinetic BIACORE measurements. Using competition BIACORE, the K_D of the wt receptor for A6 scFv was 12 ± 0.6 nM (Figure 8). This value agrees very well with values determined for A6 by equilibrium and kinetic BIACORE measurements (*2*, *9*). By competition BIACORE, the K_D of the single E55P mutant for A6 scFv was 20 ± 5 pM (Figure 8), which represents an increase in affinity of 600-fold ($\Delta\Delta G = -3.7$ kcal/mol). Four other mutants isolated from library 3 were analyzed in the same way and gave K_Ds in the same range (Table 3). A visual comparison of binding curves from BIAcore measurements (not shown) with the wt and the five receptor mutants, under comparable conditions, show that all have similar on-rates (k_{on}) with A6, but that all mutants have a much slower dissociation rate (k_{off}). The large increase in affinity, therefore, arises mainly due to the slower off-rates.

To set this result in context, single mutations that improve protein−protein binding have often been found in studies of both antibody−antigen and growth factor−receptor complexes, although typically the increases in affinity are around a factor of 10 or less. Only infrequently have larger affinity improvements arising from a single mutation been observed. Although the affinity maturation of antibodies is not strictly comparable to the strategy followed here, during somatic mutation leading to the anti-lysozyme antibody D1.3, a single change resulted in a 30-fold increase in affinity (*47*). Larger increases in antibody−protein antigen affinity typically occur only through multiple mutations. For example, affinity increases of 1230- and 420-fold were seen during maturation of antibodies against the tumor antigen c-erbB-2 (*48*) and gp120 (*49*), respectively. The 600-fold increase in antigen affinity seen here with the E55P mutant is one of the largest increases in affinity reported so far arising from a single point mutation at any protein−protein interface.

The increased affinity for A6 caused by the E55P mutation cannot be explained by extra hydrophobic contacts made by Pro at the interface. The most likely origin of the increase in binding energy (~3.7 kcal/mol) would seem to be a change in the conformation or dynamics of the epitope on the receptor. It is also possible that small changes in allowed conformation may lead to an optimization of other interactions (e.g., electrostatic) at the A6-IFNγR interface. A more detailed explanation requires knowledge of the three-dimensional structure of the mutant receptor−A6 complex, which is currently under investigation. Finally, the E55P mutation was also shown to essentially abolish binding of the natural ligand IFNγ to the receptor, again most likely due to a change in the preferred conformation of this important receptor recognition loop.

The importance of individual interactions at the A6-IFNγR interface should be amenable to analysis using double mutant cycles. A practical limitation is the difficulty of accurately measuring the low binding affinities of double mutants (J.X., unpublished work). However, using the receptor E55P mutant as a starting point for double mutant cycles may allow a more accurate estimation of binding constants for all mutant combinations, assuming that the interface is largely unperturbed. Details of these double mutant cycles, as well as more detailed crystallographic studies of the complexes, in particular to determine the structural consequences of changing large aromatic residues to alanine at this interface, will be the subject of future work.

ACKNOWLEDGMENT

The authors thank Annelies Meier for expert technical assistance.

SUPPORTING INFORMATION AVAILABLE

Table of the sequences of PCR primers and oligonucleotides used to prepare the libraries of random mutants. This material is available free of charge via the Internet at http://pubs.acs.org.

REFERENCES

1. Aguet, M., and Merlin, G. (1987) *J. Exp. Med. 165*, 988−999.
2. Sogabe, S., Stuart, F., Henke, C., Bridges, A., Williams, G., Birch, A., Winkler, F. K., and Robinson, J. A. (1997) *J. Mol. Biol. 273*, 882−897.
3. Walter, M. R., Windsor, W., Nagabhushan, T. L., Lundell, D. J., Lunn, C. A., Zauodny, P. J., and Narula, S. K. (1995) *Nature 376*, 230−235.
4. Mian, I. S., Bradwell, A. R., and Olson, A. J. (1991) *J. Mol. Biol. 217*, 133−151.
5. Padlan, E. A. (1990) *Proteins 7*, 112−124.
6. Bogan, A. A., and Thorn, K. S. (1998) *J. Mol. Biol. 280*, 1−9.
7. Jackson, R. M. (1999) *Protein Sci. 8*, 603−613.
8. LoConte, L., Chothia, C., and Janin, J. (1999) *J. Mol. Biol. 285*, 2177−2198.
9. Hofstädter, K., Stuart, F., Jiang, L., Vrijbloed, J. W., and Robinson, J. A. (1999) *J. Mol. Biol. 285*, 805−815.
10. Cunningham, B. C., and Wells, J. A. (1989) *Science 244*, 1081−1085.
11. Ausubel, F. M., Brent, R., Kingston, R. E., Moore, D. D., Seidman, J. G., Smith, J. A., and Struhl, K., Eds. (1987) *Current Protocols in Molecular Biology*, J. Wiley & Sons.

12. Hoogenboom, H. R., Griffiths, A. D., Johnson, K. S., Chiswell, D. J., Hudson, P., and Winter, G. (1991) *Nucleic Acids Res. 19*, 4133−4137.
13. Bridges, A., Stuart, F., Späth, J., Lang, S., Henke, C., Birch, A., and Robinson, J. A. (1996) *Protein Eng. 9*, 365−370.
14. Bridges, A., Birch, A., Williams, G., Aguet, M., Schlatter, D., Huber, W., Garotta, G., and Robinson, J. A. (1995) *Mol. Immunol. 32*, 1329−1338.
15. Bothmann, H., and Plückthun, A. (1998) *Nat. Biotech. 16*, 376−380.
16. Williams, G., Ruegg, N., Birch, A., Weber, C., Hofstadter, K., Robinson, J. A., Aguet, M., Garotta, G., Schlatter, D., and Huber, W. (1995) *Biochemistry 34*, 1787−1797.
17. Karlsson, R., Michaelsson, A., and Mattsson, L. (1991) *J. Immunol. Methods 145*, 229−240.
18. Schuck, P. (1997) *Annu. Rev. Biophys. Biomol. Struct. 26*, 541−566.
19. Karlsson, R., and Falt, A. (1997) *J. Immunol. Methods 200*, 121−133.
20. Griffiths, A. D., Malmqvist, M., Marks, J. D., Bye, J. M., J., E. M., McCafferty, J., Baier, M., Holliger, K. P., Gorick, B. D., Hughes-Jones, N. C., Hoogenboom, H. R., and Winter, G. (1993) *EMBO J. 12*, 725−734.
21. Sambrook, J., Fritsh, E. F., and Maniatis, T. (1989) *Molecular Cloning: A Laboratory Manual*, Cold Spring Harbor Laboratory Press, Plainview, NY.
22. Nieba, L., Krebber, A., and Plückthun, A. (1996) *Anal. Biochem. 234*, 155−165.
23. Evan, G. I., Lewis, G. K., Ramsay, G., and Bishop, J. M. (1985) *Mol. Cell. Biol. 5*, 3610−3616.
24. Desplancq, D., King, D. J., Lawson, A. D. G., and Mountain, A. (1994) *Protein Eng. 7*, 1027−1033.
25. Essig, N. Z., Wood, J. F., Howard, A. J., Raag, R., and Whitlow, M. (1993) *J. Mol. Biol. 234*, 897−901.
26. Holliger, P., Prospero, T., and Winter, G. (1993) *Proc. Natl. Acad. Sci. U.S.A. 90*, 6444−6448.
27. Kortt, A. A., Malby, R. L., Caldwell, J. B., Gruen, L. C., Ivancic, N., Lawrence, M. C., Howlett, G. J., Webster, R. G., Hudson, P. J., and Colman, P. M. (1994) *Eur. J. Biochem. 221*, 151−157.
28. Whitlow, M., Bell, B. A., Feng, S.-L., Filpula, D., Hardman, K. D., Hubert, S. L., Rollence, M. L., Wood, J. F., Schott, M. E., Milenic, D. E., Yokota, T., and Schlom, J. (1993) *Protein Eng. 6*, 989−995.
29. Whitlow, M., Filpula, D., Rollence, M. L., Feng, S. L., and Wood, J. F. (1994) *Protein Eng. 7*, 1017−1026.
30. Fasman, G. D., Ed. (1996) *Circular Dichroism and the Conformational Analysis of Biomolecules*, Plenum Press, New York.
31. MacKenzie, C. R., Hirama, T., Deng, S.-j., Bundle, D. R., Narang, S. A., and Young, N. M. (1996) *J. Biol. Chem. 271*, 1527−1533.
32. Döbeli, H., Gentz, R., Jucker, W., Garotta, G., Hartmann, D. W., and Hochuli, E. (1988) *J. Biotechnol. 7*, 199−216.
33. Gallivan, J. P., and Dougherty, D. A. (1999) *Proc. Natl. Acad. Sci. U.S.A. 96*, 9459−9464.
34. McGaughey, G. B., Gagne, M., and Rappé, A. K. (1998) *J. Biol. Chem. 273*, 15458−15463.
35. Chipot, C., Jaffe, R., Maigret, B., Pearlman, D. A., and Kollman, P. A. (1996) *J. Am. Chem. Soc. 118*, 11217−11224.
36. Rajpal, A., Taylor, M. G., and Kirsch, J. F. (1998) *Protein Sci. 7*, 1868−1874.
37. Clackson, T., and Wells, J. A. (1995) *Science 267*, 383−386.
38. Dall'Acqua, W., Goldman, E. R., Eisenstein, E., and Mariuzza, R. A. (1996) *Biochemistry 35*, 9667−9676.
39. Dall′Acqua, W., Goldman, E. R., Lin, W., Teng, C., Tsuchiya, D., Li, H., Ysern, X., Braden, B. C., Li, Y., Smith-Gill, S. J., and Mariuzza, R. A. (1998) *Biochemistry 37*, 7981−7991.
40. Pons, J., Rajpal, A., and Kirsch, J. F. (1999) *Protein Sci. 8*, 958−968.
41. Rajpal, A., Taylor, M. G., and Kirsch, J. F. (1998) *Protein Sci. 7*, 1868−1874.
42. Tsumoto, K., Ueda, Y., Maenaka, K., Watanabe, K., Ogasahara, K., Yutani, K., and Kumagai, I. (1994) *J. Biol. Chem. 269*, 28777−28782.
43. Tsumoto, K., Ogasahara, K., Ueda, Y., Watanabe, K., Yutani, K., and Kumagai, I. (1995) *J. Biol. Chem. 270*, 18551−18557.
44. Tsumoto, K., Ogasahara, K., Ueda, Y., Watanabe, K., Yutani, K., and Kumagai, I. (1996) *J. Biol. Chem. 271*, 32612−32616.
45. Goldman, E. R., Dall'Acqua, W., Braden, B. C., and Mariuzza, R. A. (1997) *Biochemistry 36*, 49−56.
46. Muller, Y. A., Chen, Y., Christinger, H. W., Li, B., Cunningham, B. C., Lowman, H. B., and deVos, A. M. (1998) *Structure 6*, 1153−1167.
47. England, P., Nageotte, R., Renard, M., Page, A.-L., and Bedouelle, H. (1999) *J. Immunol. 162*, 2129−2136.
48. Schier, R., Mccall, A., Adams, G. P., Marshall, K. W., Merritt, H., Yim, M., Crawford, R. S., Weiner, L. M., Marks, C., and Marks, J. D. (1996) *J. Mol. Biol. 263*, 551−567.
49. Yang, W. P., Green, K., Pinzsweeney, S., Briones, A. T., Burton, D. R., and Barbas, C. F. (1995) *J. Mol. Biol. 254*, 392−403.

BI000838Z